Data-Driven Model-Free Adaptive Sliding Mode Control for Multi DC Motor Speed Regulation

bim

Abstract

This paper proposes the distributed data-driven model-free adaptive sliding mode control approach to address the consensus problem of nonlinear multi-agent systems. Firstly, the equivalent data model for each agent is constructed using the compact-form dynamic linearization (CFDL) technique. Secondly, by utilizing process information from neighboring agents, the novel sliding surface is employed to ensure the boundedness of distributed measurement error. Subsequently, a distributed model-free adaptive sliding mode controller is developed for accurate consensus tracking. Finally, the effectiveness of the proposed control approach is verified through experiments on multi DC motor system.

KEYWORDS

Data-driven control, model-free adaptive sliding mode control, nonlinear multi-agent systems, multi DC motor speed control.

I. INTRODUCTION

Despite their effectiveness in certain scenarios, traditional control strategies [10]–[13] heavily depend on precise system models, and the modeling process becomes increasingly challenging as technology grows rapidly. Under such circumstances, it becomes difficult to solve practical problems using the above schemes. In modern industrial environments, vast amounts of process information often containing implicit and complex dynamic behaviors of the system are continuously generated and stored during operation. As a result, there has been a growing interest in alternative control methods that rely on data modeling.

Therefore, how to use this data to achieve system consensus control has become a powerful new topic. The data-driven control [17]–[20] refers to control systems utilizing system I/O data solely. Various data-based approaches have been developed, including model-free adaptive control, iterative learning control, virtual reference feedback tuning [21], PID control [22] and others. Among these, the model-free adaptive control approach [23]–[25] has been proposed, and has a great significance in addressing the aforementioned challenges. The design process relies solely on I/O data of the system, significantly avoiding the reliance on mathematical models. The algorithm has proven effective in practical domains such as motor systems, chemical industries, and machinery, demonstrating the adaptability and usefulness of the algorithm.

Alternatively, sliding mode control [26] has emerged as a highly attractive approach for control researchers due to the robustness to parameter uncertainties and the capability to ensure fast responses. Currently, a novel sliding mode control method based on I/O data is presented in [27], which eliminates the need for explicit system models. Although considerable progress has been made in controlling nonlinear MASs, the dynamic couplings and complex nonlinear behaviors among agents [14] can be challenging in practical implementation.

However, the effectiveness of existing approaches [31]–[34] is limited in highly uncertain environments because they typically rely on input-affine structures with known or partially known dynamics. How to achieve consensus tracking problem utilizing the model-free adaptive sliding mode controller approach for nonlinear MASs remains an open question.

Inspired by the above discussions, this paper proposes a data-driven model-free adaptive sliding mode control scheme. The contributions of this paper are structured as follows:

1) This paper establishes the model-free adaptive sliding mode control approach, which enables consensus tracking in nonlinear MASs, even under system uncertainties and unknown dynamics.
2) The method utilizes CFDL to construct equivalent data models based purely on input-output data. This allows for the systematic design of controllers for each agent without requiring internal system knowledge, making it highly practical for real-time applications.
3) A novel distributed sliding surface is developed using neighboring agent process data. This structure ensures the boundedness of measurement errors and enhances the robustness and convergence of the system through a designed stability mechanism.

The following sections will outline the remaining content of this paper: Section II provides the preliminaries and problem formulation, Section III presents the main results, Section IV shows simulation results and performance analysis, demonstrating the effectiveness of the proposed method under distinct operating conditions. At the end, conclusions are summarized in Section V.

II. Preliminaries and problem formulation

A. Directed Graph Theory

The directed graph $\mathcal{G} = (\mathcal{V}, \mathcal{E}, \mathcal{A})$ is employed to describe the information exchange between agents. Here, $\mathcal{A} = [a_{ij}] \in \mathbb{R}^{N\times N}$ represents the adjacency matrix, $\mathcal{V} = \{v_1, v_2, \ldots, v_N\}$ is the set of vertices, and $\mathcal{E} = [(v_j, v_i)|v_i \in \mathcal{V}] \subseteq \mathcal{V} \times \mathcal{V}$ is the set of edges. Moreover, $\mathcal{N}(i) = \{j \in \mathcal{V}|(i,j) \in \mathcal{E}\}$ denotes the neighbor set of agent i, where $a_{ij} \neq 0$. No self-loop is allowed in this article, which means $(i,i) \notin \mathcal{E}$ for any $i \in \mathcal{V}$, $a_{ii} = 0$. Furthermore, the degree matrix $K = diag(k_1, \ldots, k_N)$. If $k_i > 0$, agent i can directly obtain the information from the leader. The Laplacian matrix L is defined as $L = (\mathcal{D} - \mathcal{A})$, here $\mathcal{D} = diag(d_1, \ldots, d_N)$ and $d_i = \sum_{j=1}^{N} a_{ij}$ denotes the in-degree matrix. Moreover, the graph is strongly connected if the path exists between every pair of vertices.

B. Problem Formulation

Consider the nonlinear multi-agent systems composed of N agents:

$$y_i(k+1) = f_i(y_i(k), u_i(k)), \quad i = 1, 2, \ldots, N \tag{1}$$

where $u_i(k) \in \mathbb{R}$ and $y_i(k) \in \mathbb{R}$ represent the system input and output signals of agent i, respectively. $f_i(\cdot)$ signifies an unknown nonlinear function.

Assumption 1: The partial derivative of $f_i(\cdot)$ with respect to $u_i(k)$ is continuous.

Assumption 2: The system (1) satisfies the generalized Lipschitz condition, meaning that if $\Delta u_i(k) = u_i(k) - u_i(k-1) \neq 0$ then $|\Delta y_i(k+1)| \leq b|\Delta u_i(k)|$ holds for any k, where $\Delta y_i(k+1) = y_i(k+1) - y_i(k)$.

Remark 1: The assumptions above are general and commonly adopted in data-driven control. Specifically, Assumption 1 is a general condition for controller design. Assumption 2 implies that the system input variation rate constrains the rate of change of the system output. This assumption ensures that the system response to fast changing inputs remains stable and bounded, which is crucial for the design of adaptive control strategies.

Assumption 3: The communication graph $\mathcal{G}$ is strongly connected, ensuring that each follower can directly receive information from at least one leader.

Lemma 1 [8]: Consider the nonlinear multi-agent system (1) satisfying above three assumptions. If $|\Delta u_i(k)| \neq 0$ holds, then the system can be transformed into the CFDL data model as follows:

$$\Delta y_i(k+1) = \phi_i(k)\Delta u_i(k) \tag{2}$$

wherein $\phi_i(k)$ is called pseudo partial derivative (PPD), satisfying $|\phi_i(k)| \leq b$.

The distributed measurement error of $\xi_i(k)$ for N agents is established as:

$$\xi_i(k) = \sum_{j \in N_i} a_{ij}(y_j(k) - y_i(k)) + d_i(y_d(k) - y_i(k)) \tag{3}$$

if the agent i can receive data from the leader, then $d_i = 1$; otherwise, $d_i = 0$. Additionally, $y_d(k)$ represents the reference trajectory.

Remark 2: The CFDL technique requires no prior knowledge about the system dynamic model, making it highly suitable for distributed multi-agent systems, which often exhibit complex, nonlinear, and time-varying dynamics that are difficult to model accurately due to the heterogeneous agents. In addition, CFDL is effective in handling complex systems where modeling is impractical. Moreover, the dynamic behavior of time-varying PPD may be highly complex, which is challenging to verify. Consequently, a data-driven control method is employed to adaptively study the dynamic behavior, which ensures effective control performance.

III. Main Results

This section is devided in two parts. The first part introduces the model-free adaptive controller design, which is based on the CFDL technique. The second part introduces the sliding mode controller design, which is formulated based on the distributed measurement error. The overall block diagram of the proposed control scheme is shown in Fig. 1.

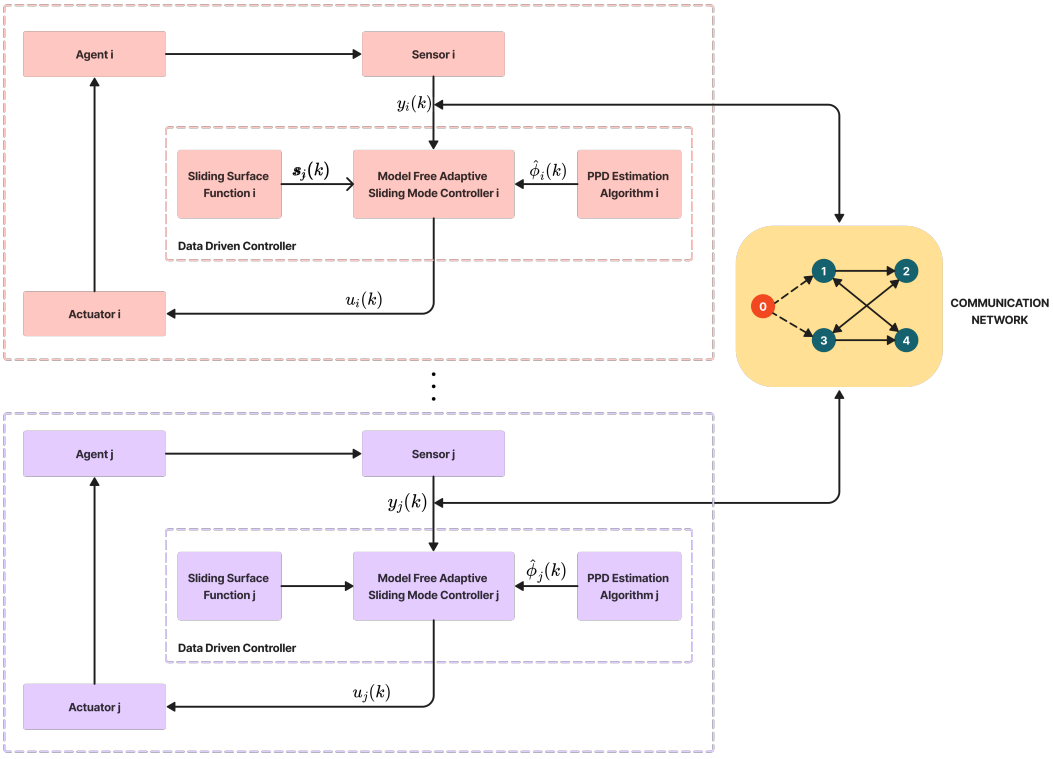

Fig. 1: Block diagram.

A. Model-Free Adaptive Sliding Mode Controller Design

Consider the following PPD criterion function for the parameter with unknown dynamics in (2):

$$J(\phi_i(k)) = |\Delta y_i(k) - \phi_i(k)\Delta u_i(k-1)|^2 + \mu|\phi_i(k) - \hat{\phi}_i(k-1)|^2 \tag{4}$$

By utilizing the optimal condition $\frac{\partial J(\phi_i(k))}{\partial \phi_i(k)} = 0$, the updating law with reset algorithm is derived:

$$\hat{\phi}_i(k) = \hat{\phi}_i(k-1) + \frac{\eta \Delta u_i(k-1)}{\mu + \Delta u_i(k-1)^2}(\Delta y_i(k) - \hat{\phi}_i(k-1)\Delta u_i(k-1)) \tag{5}$$

$$\hat{\phi}_i(k) = \hat{\phi}_i(1), \text{ if } |\hat{\phi}_i(k)| \leq \epsilon \ or \ sign(\hat{\phi}_i(k)) \neq sign(\hat{\phi}_i(1)) \tag{6}$$

herein, $\eta \in (0,1)$, $\mu > 0$ represents a positive weight factor. Additionally, ϵ is a small positive number and $\hat{\phi}_i(k)$ signifies the estimated value of $\phi_i(k)$.

The following distributed MFAC algorithm is presented:

$$u_{i,\text{MFA}}(k) = u_{i,\text{MFA}}(k-1) + \frac{\rho \hat{\phi}_i(k)}{\lambda + \hat{\phi}_i(k)^2}\xi_i(k) \tag{7}$$

where $\rho \in$ (0,1) is a step-size constant, which is added to make (7) general.

To design the sliding mode controller, the sliding surface function is given by:

$$s_i(k) = \alpha \xi_i(k) - \xi_i(k-1) \tag{8}$$

herein $\alpha > 1$ represents a positive constant.

Furthermore, from (2) and (3), the formula (3) is updated as

$$\xi_i(k+1) = \xi_i(k) - (\sum_{j \in N_i} a_{ij} + d_i)\phi_i(k)\Delta u_i(k) + \sum_{j \in N_i} a_{ij}\Delta y_j(k) + d_i \Delta y_d(k+1) \tag{9}$$

wherein $\Delta y_j(k+1)$ is replaced with $\Delta y_j(k)$ because the data at the next moment cannot be obtained.

Therefore, with the assistance of reaching law $s_i(k+1) = 0$, the following equivalent control law can be derived.

$$\Delta u_{i,\text{SM}}^{eq} = \frac{\omega \hat{\phi}_i(k)}{\sigma + \hat{\phi}_i(k)^2}\left(\frac{\xi_i(k) + \sum_{j \in N_i} a_{ij}\Delta y_j(k) + d_i \Delta y_d(k+1)}{\sum\limits_{j \in N_i} a_{ij} + d_i} - \frac{\xi_i(k)}{\alpha(\sum\limits_{j \in N_i} a_{ij} + d_i)}\right) \tag{10}$$

The controller consists of an equivalent control law and switching control law, which means:

$$u_{i,\text{SM}}(k) = u_{i,\text{SM}}(k-1) + \Delta u_{i,\text{SM}}^{M}(k) + \Delta u_{i,\text{SM}}^{s}(k) \tag{11}$$

Additionally, the switching control law $\Delta u_{i,\text{SM}}^{s}(k)$ is presented:

$$\Delta u_{i,\text{SM}}^{s}(k) = \frac{\omega \hat{\phi}_i(k)}{\sigma + \hat{\phi}_i(k)^2}\tau_s sign(s_i(k)) \tag{12}$$

As a consequence, taking into consideration (10), (11) and (12), the controller is summarized as follows:

$$\begin{aligned} u_{i,\text{SM}}(k) = u_{i,\text{SM}}(k-1) + \frac{\omega \hat{\phi}_i(k)}{\sigma + \hat{\phi}_i(k)^2}\Bigg(&\frac{\xi_i(k) + \sum_{j \in N_i} a_{ij}\Delta y_j(k) + d_i \Delta y_d(k+1)}{\sum_{j \in N_i} a_{ij} + d_i} \\ &- \frac{\xi_i(k)}{\alpha(\sum\limits_{j \in N_i} a_{ij} + d_i)} + \tau_s sign(s_i(k))\Bigg) \end{aligned} \tag{13}$$

Subsequently, the final input is:

$$u_i(k) = u_{i,\text{MFA}}(k) + \Gamma_i u_{i,\text{SM}}(k) \tag{14}$$

where the parameter Γ_i is a gain factor.

B. Stability Analysis

Theorem 1: For the system (1) satisfying assumptions 1-3, using the designed algorithms (5) along with the reset law (6), the sliding surface (8) and controller (13) can ensure the boundedness of $\hat{\phi}_i(k)$. Simultaneously, the distributed measurement error remains bounded.

Proof: The proof is divided into two parts, which are addressed respectively.

Part i: Define $\tilde{\phi}_i(k) = \hat{\phi}_i(k) - \phi_i(k)$. Using the PPD estimation algorithm (5), the following result is derived:

$$\begin{aligned}
\tilde{\phi}_i(k) &= \big(\hat{\phi}_i(k-1) - \phi_i(k-1)\big) + \frac{\eta \Delta u_i(k-1)}{\mu + \Delta u_i(k-1)^2}\big(\phi_i(k-1)\Delta u_i(k-1) \\
&- \hat{\phi}_i(k-1)\Delta u_i(k-1)\big) - \phi_i(k) + \phi_i(k-1) \\
&= \tilde{\phi}_i(k-1) + \frac{\eta \Delta u_i(k-1)}{\mu + \Delta u_i(k-1)^2}\big(\phi_i(k-1)\Delta u_i(k-1) \\
&- \hat{\phi}_i(k-1)\Delta u_i(k-1)\big) - \phi_i(k) + \phi_i(k-1) \\
&= \tilde{\phi}_i(k-1) + \frac{\eta \Delta u_i(k-1)}{\mu + \Delta u_i(k-1)^2}\Delta u_i(k-1)\big(\phi_i(k-1) - \hat{\phi}_i(k-1)\big) - \phi_i(k) + \phi_i(k-1) \\
&= \left(1 - \frac{\eta \Delta u_i(k-1)^2}{\mu + \Delta u_i(k-1)^2}\right)\tilde{\phi}_i(k-1) - \Delta\phi_i(k)
\end{aligned} \tag{15}$$

Denote that the term $\frac{\eta \Delta u_i(k-1)^2}{\mu + \Delta u_i(k-1)^2}$ is monotonically increasing with respect to $\Delta u_i(k)^2$, and its minimum value is $\frac{\eta \epsilon^2}{\mu + \epsilon^2}$. Therefore, there must be a constant q_1 satisfying the inequalities $0 < \eta \leq 1$ and $u_i > 0$

$$0 < \left|1 - \frac{\eta \Delta u_i(k-1)^2}{\mu + \Delta u_i(k-1)^2}\right| \leq 1 - \frac{\eta \epsilon^2}{\mu + \epsilon^2} = q_1 < 1 \tag{16}$$

Because of $|\phi_i(k)| < \bar{d}$, and $|\Delta\phi_i(k)| < 2\bar{d}$, the following equation (15) is written as:

$$\begin{aligned}
|\tilde{\phi}_i(k)| &\leq q_1|\tilde{\phi}_i(k-1)| + 2\bar{d} \\
&\leq q_1^2|\tilde{\phi}_i(k-2)| + 2q_1\bar{d} + 2\bar{d} \\
&\vdots \\
&\leq q_1^{k-1}|\tilde{\phi}_i(1)| + \frac{2\bar{d}}{1-q_1}(1 - q_1^{k-1})
\end{aligned} \tag{17}$$

which implies $\tilde{\phi}_i(k)$ is bounded. Since the boundedness of $\phi_i(k)$ is guaranteed by Lemma 1.

Part ii: The boundedness of $\xi_i(k)$.

By combining (5) with (9), the expression for $\xi_i(k+1)$ is updated:

$$\begin{aligned}
\xi_i(k+1) &= \xi_i(k) + \sum_{j \in N_i} a_{ij}\Delta y_j(k) + d_i\Delta y_d(k+1) - \frac{\omega\phi_i(k)\hat{\phi}_i(k)}{\sigma + \hat{\phi}_i(k)^2}\big(1 - \frac{1}{\alpha}\big)\xi_i(k) \\
&- \frac{\omega\phi_i(k)\hat{\phi}_i(k)}{\sigma + \hat{\phi}_i(k)^2}\sum_{j \in N_i} a_{ij}\Delta y_j(k) - \frac{\omega\phi_i(k)\hat{\phi}_i(k)}{\sigma + \hat{\phi}_i(k)^2}d_i\Delta y_d(k+1) + \Big(\sum_{j \in N_i} a_{ij} + d_i\Big)\tau_s\,\mathrm{sign}(s_i(k)) \\
&= \left(1 - \frac{\omega\phi_i(k)\hat{\phi}_i(k)}{\sigma + \hat{\phi}_i(k)^2}\big(1 - \frac{1}{\alpha}\big)\right)\xi_i(k) + \left(\sum_{j \in N_i} a_{ij}\Delta y_j(k) - \frac{\omega\phi_i(k)\hat{\phi}_i(k)}{\sigma + \hat{\phi}_i(k)^2}\sum_{j \in N_i} a_{ij}\Delta y_j(k)\right) \\
&+ \left(d_i\Delta y_d(k+1) - \frac{\omega\phi_i(k)\hat{\phi}_i(k)}{\sigma + \hat{\phi}_i(k)^2}d_i\Delta y_d(k+1)\right) + \Big(\sum_{j \in N_i} a_{ij} + d_i\Big)\tau_s\,\mathrm{sign}(s_i(k)) \\
&= \left(1 - \frac{\omega\phi_i(k)\hat{\phi}_i(k)}{\sigma + \hat{\phi}_i(k)^2}\big(1 - \frac{1}{\alpha}\big)\right)\xi_i(k) + \left(1 - \frac{\omega\phi_i(k)\hat{\phi}_i(k)}{\sigma + \hat{\phi}_i(k)^2}\right)\Big(\sum_{j \in N_i} a_{ij}\Delta y_j(k)
\end{aligned}$$

$$+ d_i \Delta y_d(k+1)\Big) - \frac{\omega \phi_i(k)\hat{\phi}_i(k)}{\sigma + \hat{\phi}_i(k)^2}\Big(\sum_{j\in N_i} a_{ij} + d_i\Big)\tau_s \,\mathrm{sign}(s_i(k)) \tag{18}$$

Subsequently, take $0 < h_0 < h_i(k) < \frac{\omega C_0}{2\sqrt{\sigma}} < 1$ into consideration, where $\phi_i(k) < C_0$ and $|g_i(k)| < g_0$, the inequality is obtained by taking the absolute value of each term of (18).

$$\begin{aligned} |\xi_i(k+1)| &\le |1 - h_i(k)(1-\frac{1}{\alpha})||\xi_i(k)| + |g_i(k)| \\ &\le |1 - h_i(k)(1-\frac{1}{\alpha})||\xi_i(k)| + g_0(k) \\ &\vdots \\ &\le 1 - h_0(1-\frac{1}{\alpha})^k |\xi_i(0)| + \frac{g_0(1-(1-h_0(1-\frac{1}{\alpha}))^2)}{h_0(1-\frac{1}{\alpha})} \end{aligned} \tag{19}$$

Therefore, the following result will be given as

$$\lim_{k\to\infty} \xi_i(k) = \frac{\alpha g_0}{(\alpha - 1)h_0} \tag{20}$$

In summary, both the parameter estimation $\hat{\phi}_i(k)$ and the measurement error $\xi_i(k)$ remain bounded under the proposed adaptive sliding mode control scheme. The condition $0 < h_0 < h_i(k) < \frac{\omega C_0}{2\sqrt{\sigma}} < 1$ ensures that the adaptive parameters are stable, thereby enabling effective performance of the distributed controller. This completes the proof.

Remark 3: Unlike the consensus tracking control schemes used in the existing literature, this paper proposes a model-free adaptive sliding mode control strategy for MASs. The introduced approach leverages the CFDL technique alongside a novel sliding surface, relying solely on data to accurately track the reference trajectory tracking.

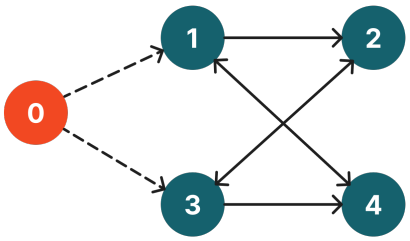

Fig. 2: Communication topology among agents.

IV. Simulation Example

This section describes the usefulness of the provided control approach, which is validated by both numerical simulations and physical experiments results. The DC brushed motors operate at 12V with a no-load speed of 293±21RPM and a gear ratio of 20, providing increased torque. Hall encoders with 13 pulses per revolution are used to capture rotor motion. The motor speed is measured in revolutions per second (r/s) based on encoder measurements and the sampling interval t. The total number of encoder counts per revolution is calculated as $rT = 4N_e Rr$, where N_e is the encoder line count equal to 13, R_r is the reduction ratio equal to 20. The number of rotations is determined using $N_r = \frac{m}{rT}$, with m representing the total encoder count. The output data model of each agent is governed by:

$$y_i(k+1) = 0.5y_i(k) + b_i u_i(k) - 0.02y_i(k)^{p_i} + 0.45, \quad i = 1,2,3,4,$$

where the parameters corresponding to each agent are:

$$b_i = \begin{cases} \frac{6m}{rT} & \text{if } i = 1,3 \\ \frac{5.75m}{rT} & \text{if } i = 2,4 \end{cases} \qquad p_i = \begin{cases} 3 & \text{if } i = 1,3 \\ 2 & \text{if } i = 2,4 \end{cases}$$

Noting that the multi-agent systems are heterogeneous, with four agents having different dynamic models. In addition, these models are not used in the control design but only serve to generate the I/O data required for the MAS simulations. As illustrated in Fig. 2, the virtual leader is designated as vertex 0. It can be observed that only agents 1 and 3 can receive information from the leader, forming a strongly connected communication graph. The Laplacian matrix of the graph is given as follows:

$$L = \begin{bmatrix} 1 & 0 & 0 & -1 \\ -1 & 2 & -1 & 0 \\ 0 & -1 & 1 & 0 \\ -1 & 0 & -1 & 2 \end{bmatrix}$$

with $D = \text{diag}(1, 0, 1, 0)$.

Example 1: In this example, the reference trajectory is time-invariant value signal $y_d(k) = 0.6$. The initial parameters are chosen as $u_i(1) = 0$, $y_i(1) = 0$ and $\hat{\phi}_i(0) = 1$ for all agents in this simulation, $\Gamma_1 = \Gamma_3 = 0.45$ and $\Gamma_2 = \Gamma_4 = 0.15$, with $\tau_s = 10^{-5}$, $m = 600$, $rT = 1024$, $\eta = 1$, $\mu = 0.005$, other parameters are given as $\rho = 7.5$, $\lambda = 350$, $\omega = 10$, $\sigma = 95$, $\alpha = 15$ with $\epsilon = 10^{-5}$.

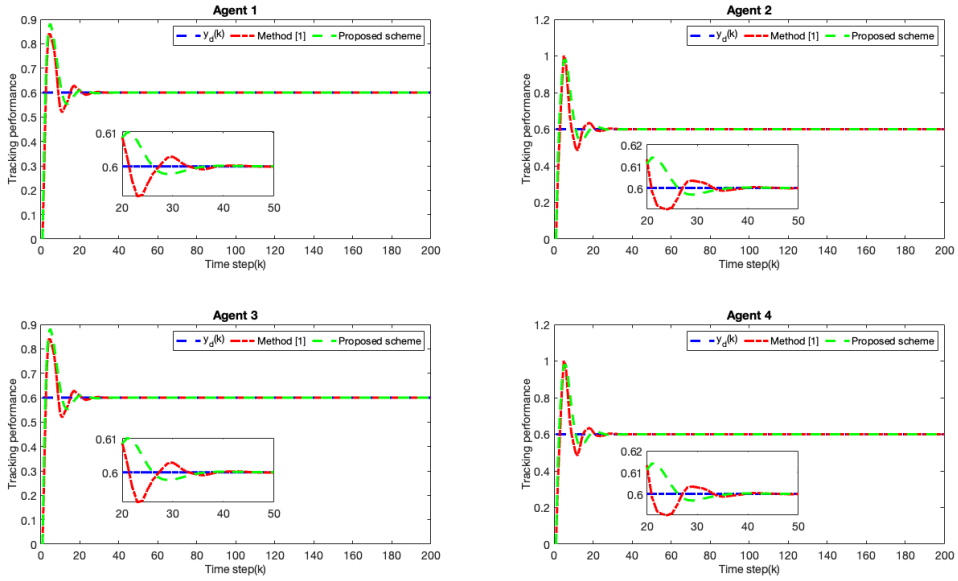

Fig. 3: Tracking performance.

Fig. 3 demonstrates the tracking performance for the time-invariant reference signal. It can be observed that all agents accurately converge to the reference trajectory. Moreover, Fig. 4 illustrates the distributed measurement errors, which remain bounded within the range of [-0.02, 0.02], indicating accuracy of the proposed control strategy.

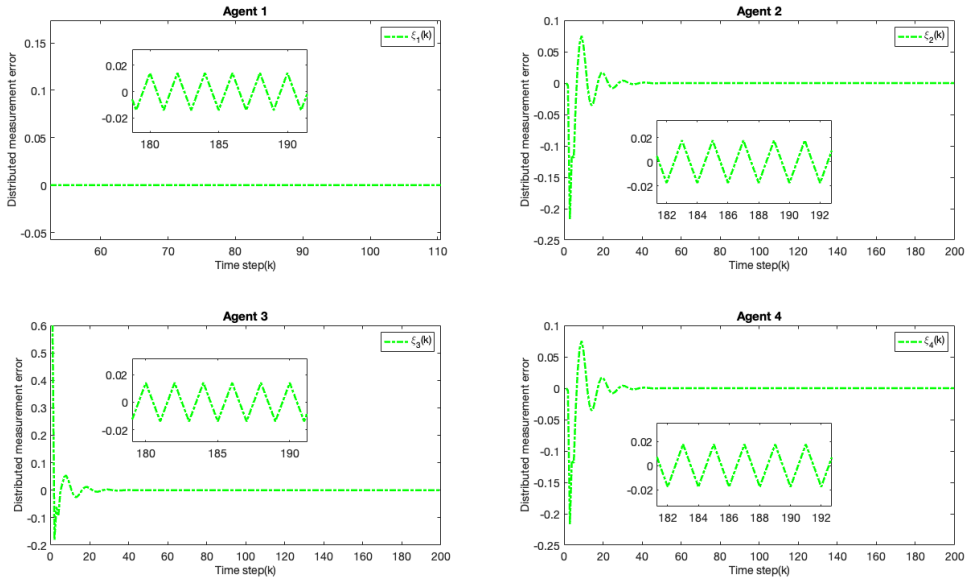

Fig. 4: Distributed measurement errors.

TABLE I: Mean square error comparison (Example 1)

$\text{MSE}_i(k)$	Method [1]	Proposed scheme
Agent 1	4.9135×10^{-3}	4.0732×10^{-3}
Agent 2	3.2197×10^{-3}	2.2558×10^{-3}
Agent 3	4.9135×10^{-3}	4.0732×10^{-3}
Agent 4	3.2197×10^{-3}	2.2558×10^{-3}
Average	4.0666×10^{-3}	3.1649×10^{-3}

To quantitatively evaluate the advantages of the developed method, the mean square error (MSE) is calculated for each agent. The MSE values are presented in TABLE I. For each agent, the MSE is calculated according to the formula:

$$\text{MSE}_i(k) = \frac{1}{m}\sum_{k=1}^{m}\xi_i^2(k)$$

where m denotes the total number of time steps. In comparison to the existing approach [1], the developed strategy demonstrates significant improvement in accuracy, reducing the average MSE across agents by a factor of approximately 1.29. This notable reduction confirms the effectiveness of the proposed technique.

Example 2: The expression for the reference trajectory is:

$$y_d(k) = 0.6\sin(0.07\pi(k)) + 0.6\cos(0.04\pi(k)), k \in [0, 200]$$

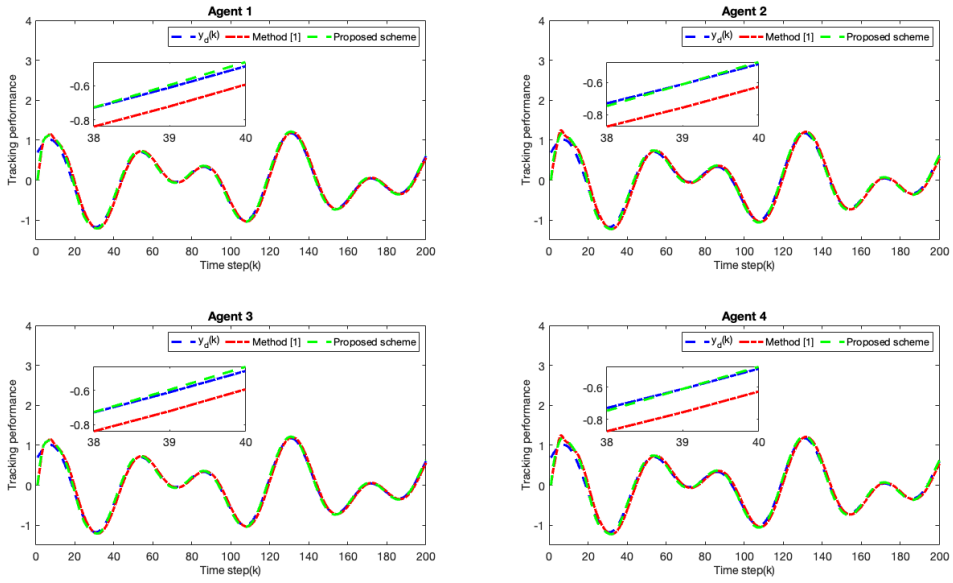

Fig. 5: Tracking performance of all agents under the time-varying reference trajectory.

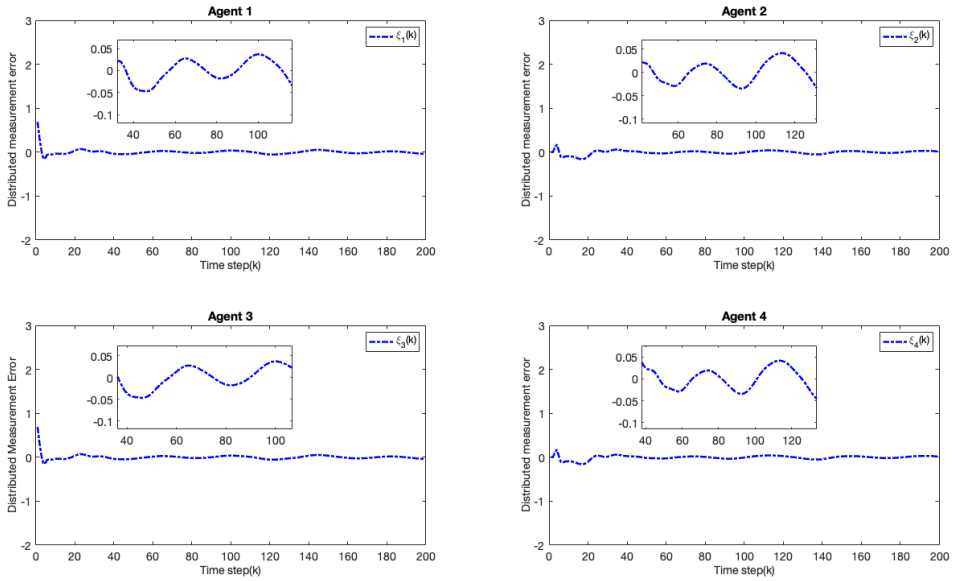

Fig. 6: Distributed measurement errors.

Fig. 5 presents the tracking performance for the time-varying trajectory. All agents are able to accurately track the reference trajectory. Additionally, as shown in Fig. 6 the distributed measurement errors among agents are bounded. For time-varying reference trajectories, the mean squared errors of distributed measurements for two control strategies are detailed in TABLE II. Relative to the conventional approach [1], the proposed scheme reduces in average MSE by approximately 1.16.

TABLE II: Mean square error comparison (Example 2)

$\text{MSE}_i(k)$	Method [1]	Proposed scheme
Agent 1	2.8319×10^{-3}	2.6984×10^{-3}
Agent 2	1.4561×10^{-3}	9.8907×10^{-4}
Agent 3	2.8319×10^{-3}	2.6984×10^{-3}
Agent 4	1.4561×10^{-3}	9.8907×10^{-4}
Average	2.1445×10^{-3}	1.8432×10^{-3}

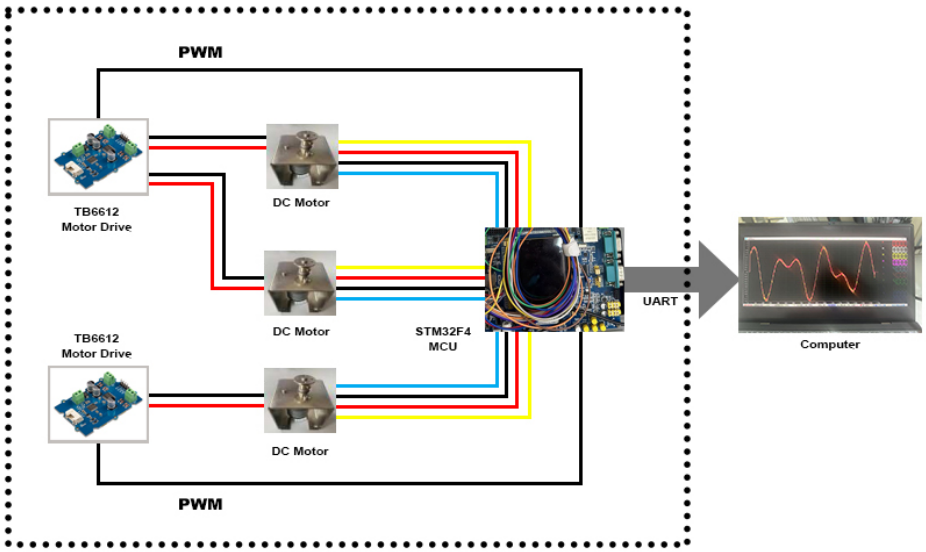

Fig. 7: System connection diagram of multi DC motor consensus tracking control.

To verify the proposed consensus tracking control methodology, the experimental validation is conducted using a multi DC motor system, as illustrated in Fig. 8. The system consists of three DC motors equipped with Hall encoders and reduction gears, an STM32F407 main control chip, two motor drive modules, and an LCD display module. The microcontroller unit STM32F407ZGT6 is used for high-resolution pulse width modulation output generation to achieve precise motor speed control. The timer module is utilized for this purpose.

In addition, the controller code is written in C language using STM32CubeIDE, while STM32CubeMX is used for pin configuration. The main purpose of the experiment is to ensure that the three motors accurately track the reference trajectory:

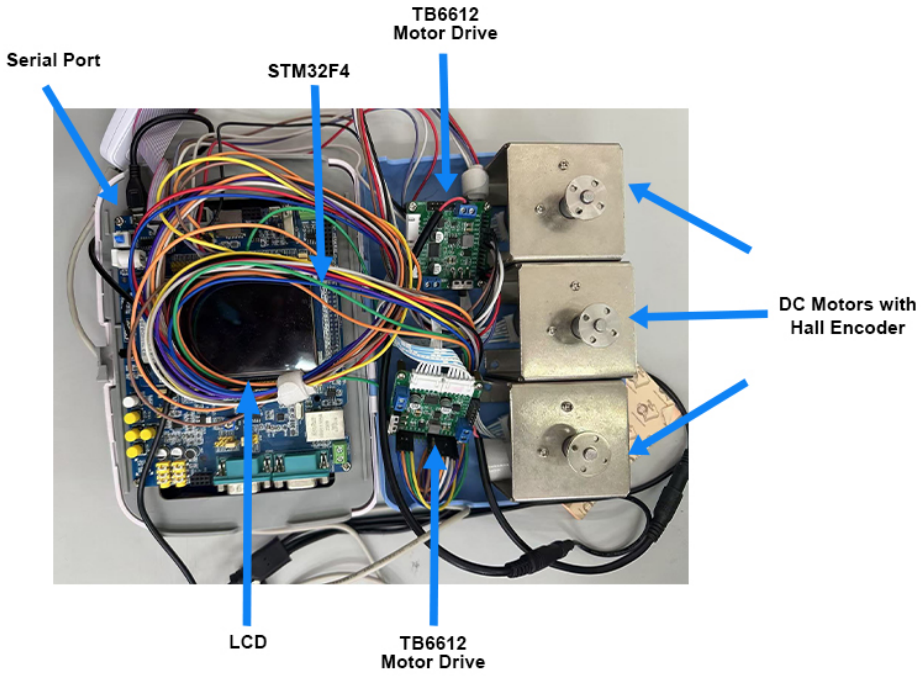

Fig. 8: Multi DC motor system.

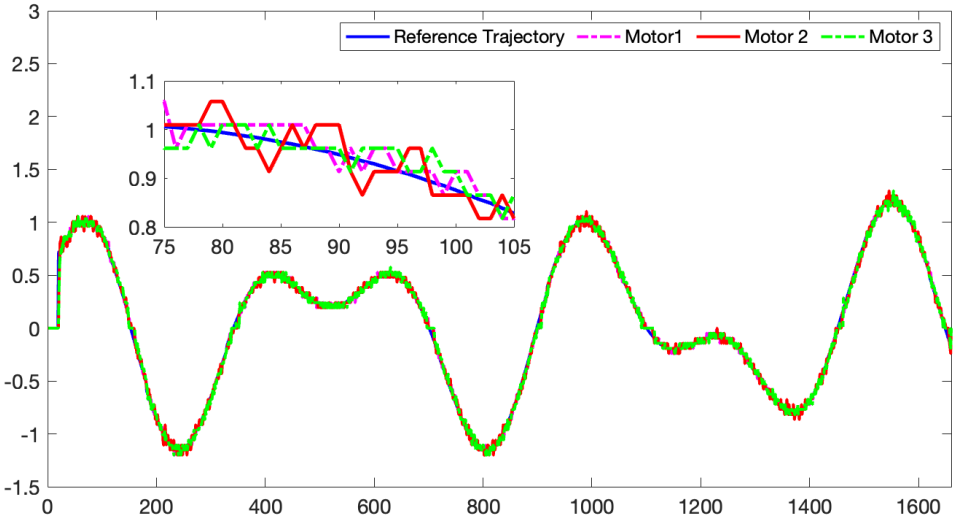

Fig. 9: Tracking performance.

Fig. 9 shows the tracking performance of multi DC motor demonstrating the effectiveness of the proposed control method. Overall, the simulation results suggest that the proposed control system is capable of tracking a constant desired trajectory for multiple agents. While initial transient errors may occur, the system ultimately achieves a steady-state condition with minimal tracking error. The variations in tracking performance among the agents highlight the potential influence of individual characteristics and external factors.

The distributed errors for three DC motors result in mean squared errors of 1.0840×10^{-3}, 1.5036×10^{-3}, and 1.4887×10^{-3}, respectively. The average of 1.3588×10^{-3} demonstrates the effectiveness of the proposed control method in practical

applications. Meanwhile, the method consistently maintains mean squared error around 10^{-3}.

Remark 4:The tracking performance is related to the key design parameters, including ρ, ω, σ, α, and the sampling period. However, the algorithm ability to address system uncertainties can be enhanced by appropriately increasing ρ and ω. Furthermore, it is necessary to make precise adjustments to other parameters, such as Γ_i and τ_s, to achieve accurate performance.

V. Conclusion

In this study, the model-free adaptive sliding mode control approach is presented to address the consensus problem of MASs. Firstly, the equivalent data model for each agent is obtained using the CFDL method. Secondly, a novel sliding surface ireas presented to ensure that the distributed measurement error remains bounded. Moreover, the developped strategy effectively mitigates the impact of distributed measurement errors across agents. The simulation results, quantitatively demonstrate the superiority of the proposed technique. Specifically, the mean squared error for each agent is calculated, revealing an average mean squared error reduction of approximately 1.29 compared to the existing approach [1], and approximately 1.16 for time-varying signals. Finally, the effectiveness of the proposed control approach is verified through physical experiments on multi DC motor system.

References

[1] X. Bu, Z. Hou, and H. Zhang, "Data-driven multiagentsystems consensus tracking using model free adaptive control," IEEE Transactions on Neural Networks and Learning Systems, vol. 29, no. 5, pp. 1514-1524, 2018.

[2] M. Parsa and M. Danesh, "Robust containment control of uncertain multi-agent systems with time-delay and heterogeneous lipschitz nonlinearity," IEEE Transactions on Systems, Man, and Cybernetics: Systems, vol. 51, no. 4, pp. 2312-2321, 2021.

[3] A.-Y. Lu and G.-H. Yang, "Distributed secure state estimation for linear systems against malicious agents throughsorting and filtering," Automatica, vol. 151, pp. 110927,2023.

[4] T. Li, W. Bai, Q. Liu, Y. Long and C. L. P. Chen, "Distributed fault tolerant containment control protocols for the discrete-time multiagent systems via reinforcement learning method," IEEE Transactions on Neural Networks and Learning Systems, vol. 34, no. 8, pp. 3979-3991, Aug. 2023

[5] Y. Yang, Y. Xiao and T. Li, "Attacks on formation control for multiagent systems," IEEE Transactions on Cybernetics, vol. 52, no. 12, pp. 12805- 12817, Dec. 2022

[6] R. Olfati-Saber, J. A. Fax, and R. M. Murray, "Consensus and cooperation in networked multi-agent systems," *Proceedings of the IEEE*, vol. 95, no. 1, pp. 215-233, 2007.

[7] M. Sampei, T. Tamura, T. Kobayashi, and N. Shibui, "Arbitrary path tracking control of articulated vehicles using nonlinear control theory," IEEE Trans. Control Syst. Technol., vol. 3, no. 1, pp. 125–131, Mar. 1995.

[8] W. Ren, R. W. Beard, and E. M. Atkins, "Information consensus in multivehicle cooperative control," *IEEE Control Systems*, vol. 27, no. 2, pp. 71-82, 2007.

[9] D. Xu, B. Jiang, and P. Shi, "Adaptive observer based data-driven control for nonlinear discrete-time processes," *IEEE Transactions on Automation Science and Engineering*, vol. 11, no. 4, pp. 1037-1045, 2014.

[10] J. Wang, X. Wang, X. Zhang, and S. Zhu, "Global h-synchronization for high-order delayed inertial neural networks via direct SORS strategy," *IEEE Transactions on Systems, Man, and Cybernetics: Systems*, vol. 53, no. 11, pp. 6693–6704, 2023.

[11] F. Xu, X. Ruan, and X. Pan, "Event-triggered leaderfollowing consensus control of multiagent systems against DoS attacks," International Journal of Control, Automation and Systems, vol. 22, pp. 3424-3433, 2024.

[12] Y. Liu, L. Liu, and S. Tong, "Adaptive neural network tracking design for a class of uncertain nonlinear discrete time systems with dead-zone," Science China Information Sciences, vol. 57, pp. 1-12, 2014.

[13] Z. Dong, X. Wang, X. Zhang, M. Hu, and T.N. Dinh, "Global exponential synchronization of discrete-time high order switched neural networks and its application to multi channel audio encryption," Nonlinear Analysis: Hybrid systems, vol. 47, pp. 101291, 2023.

[14] X. Liu, J. Lam, W. Yu, and G. Chen, "Finite-time consensus of multiagent systems with a switching protocol," *IEEE Transactions on Neural Networks and Learning Systems*, vol. 27, no. 4, pp. 853–862, Apr. 2016.

[15] Z. Hou and Z. Wang, "From model-based control to data-driven control: Survey, classification and perspective," Inf. Sci., vol. 235, pp. 3–35, 2013.

[16] Z. Hou and S. Jin, "A novel data-driven control approach for a class of discrete-time nonlinear systems," IEEE Trans. Control Syst. Technol., vol. 19, no. 6, pp. 1549–1558, Nov. 2011.

[17] Y. Asadi, M.M. Farsangi, and M.H. Rezaei, “Improved data-driven adaptive control structure against input and output saturation,” International Journal of Control, Automation and Systems, vol. 22, pp. 2981-2989, 2024.

[18] Y. Hui, R. Chi, B. Huang, Z. Hou, and S. Jin, “Observer-based sampled-data model-free adaptive control for continuous-time nonlinear nonaffine systems with input rate constraints,” IEEE Transactions on Systems, Man, and Cybernetics: Systems, vol. 51, no. 12, pp. 7813-7822, 2021.

[19] Y.-S. Ma, W.-W. Che, C. Deng, and Z.-G. Wu, “Distributed model-free adaptive control for learning nonlinear MASs under DoS attacks,” IEEE Transactions on Neural Networks and Learning Systems, vol. 34, no. 3, pp. 1146-1155, 2023.

[20] H. Wang, Q. Luo, N. Li, and W. Zheng, “Data-driven model free formation control for multi-USV system in complex marine environments,” International Journal of Control, Automation and Systems, vol. 20, pp. 3666-3677, 2022.

[21] L. Duan, Z. Hou, X. Yu, S. Jin, and K. Lu, “Data-driven model-free adaptive attitude control approach for launch vehicle with virtual reference feedback parameters tuning method,” IEEE Access, vol. 7, pp. 54106-54116, 2019.

[22] Kiam Heong Ang, G. Chong and Yun Li, “PID control system analysis, design, technology,” IEEE Transactions on Control Systems Technology, vol. 13, no. 4, pp. 559-576, Jul. 2005.

[23] P. Zhu, S. Jin, X. Bu and Z. Hou, “Improved model-free adaptive control for MIMO nonlinear systems with event-triggered transmission scheme and quantization,” IEEE Transactions on Cybernetics, vol. 53, no. 9, pp. 5867-5880, Sept. 2023.

[24] D. Xu, Y. Shi and Z. Ji, “Model-free adaptive discrete-time integral sliding-mode-constrained-control for autonomous 4WMV parking systems,” IEEE Transactions on Industrial Electronics, vol. 65, no. 1, pp. 834-843, Jan. 2018.

[25] D. Liu and G.-H. Yang, “Prescribed performance model-free adaptive integral sliding mode control for discrete-time nonlinear systems,” IEEE Transactions on Neural Networks and Learning Systems, vol. 30, no. 7, pp. 2222-2230, Jul. 2019.

[26] P. Shi, Y. Xia, G. Liu, D. Rees, On designing of sliding-mode control for stochastic jump systems, IEEE Trans. Automat. Control 51 (1) (2006) 97–103.

[27] D. Liu and G.-H. Yang, “Data-driven adaptive sliding mode control of nonlinear discrete-time systems with prescribed performance,” IEEE Transactions on Systems, Man, and Cybernetics: Systems, vol. 49, no. 12, pp. 2598-2604, 2019.

[28] Z. Wu, X. Wang, and X. Zhao, “Backstepping terminal sliding mode control of DFIG for maximal wind energy captured,” Int. J. Innovative Comput. Inf. Control, vol. 12, no. 5, pp. 1565–1579, 2016.

[29] X. Yan and C. Edwards, “Adaptive sliding-mode-observer-based fault reconstruction for nonlinear systems with parametric uncertainties,” IEEE Trans. Ind. Electron., vol. 55, no. 11, pp. 4029–4036, Nov. 2008.

[30] J. Liu, W. Luo, X. Yang, and L. Wu, “Robust model-based fault diagnosis for PEM fuel cell air-feed system,” IEEE Trans. Ind. Electron., vol. 63, no. 5, pp. 3261–3270, May 2016.

[31] A. Anuchin, A. Dianov and F. Briz, ”Synchronous Constant Elapsed Time Speed Estimation Using Incremental Encoders,” in IEEE/ASME Transactions on Mechatronics, vol. 24, no. 4, pp. 1893-1901, Aug. 2019, doi: 10.1109/TMECH.2019.2928950.

[32] S. Qin and T. Badgwell, “A survey of industrial model predictive control technology,” Control Eng. Pract., vol. 11, pp. 733–764, 2003.

[33] X. Ma, F. Sun, H. Li, and B. He, ”Neural-network-based integral sliding-mode tracking control of second-order multi-agent systems with unmatched disturbances and completely unknown dynamics,” *International Journal of Control, Automation and Systems*, vol. 15, no. 4, pp. 1925–1935, 2017.

[34] R. Rahmani, H. Toshani, and S. Mobayen, ”Consensus tracking of multi-agent systems using constrained neural-optimiser-based sliding mode control,” *International Journal of Systems Science*, vol. 51, no. 14, pp. 2653–2674, 2020.

[35] Z. Peng, G. Wen, A. Rahmani, and Y. Yongguang, ”Distributed consensus-based formation control for multiple nonholonomic mobile robots with a specified reference trajectory,” *International Journal of Systems Science*, vol. 46, no. 8, pp. 1447–1457, 2015.